

See discussions, stats, and author profiles for this publication at: <https://www.researchgate.net/publication/47792958>

# Glass Dynamics and Anomalous Aging in a Family of Ionic Liquids above the Glass Transition Temperature

ARTICLE *in* THE JOURNAL OF PHYSICAL CHEMISTRY B · NOVEMBER 2010

Impact Factor: 3.3 · DOI: 10.1021/jp1044089 · Source: PubMed

---

CITATIONS

15

READS

45

## 2 AUTHORS:



Nabila Shamim

Texas Tech University

11 PUBLICATIONS 240 CITATIONS

[SEE PROFILE](#)



Gregory B Mckenna

Texas Tech University

334 PUBLICATIONS 8,055 CITATIONS

[SEE PROFILE](#)

# Glass Dynamics and Anomalous Aging in a Family of Ionic Liquids above the Glass Transition Temperature

Nabila Shamim and Gregory B. McKenna\*

Department of Chemical Engineering, Texas Tech University, Lubbock, Texas 79409-3121, United States

Received: May 14, 2010; Revised Manuscript Received: September 11, 2010

The present paper reports the results of a systematic rheological study of the dynamic moduli of 1-butyl 3-methylimidazolium tetrafluoroborate ( $[Bmim][BF_4]$ ), 1-butyl 3-methylimidazolium hexafluorophosphate ( $[Bmim][PF_6]$ ), and 1-ethyl 3-methylimidazolium ethylsulfate ( $[Emim][EtSO_4]$ ) in the vicinity of their respective glass transition temperatures. The results show an anomalous aging in that the dynamic and the low shear rate viscosities decrease with time at temperatures near to, but above, the glass transition temperature, and this is described. The samples that are aged into equilibrium obey the time–temperature superposition principle, and the shift factors and the viscosities follow classic super-Arrhenius behaviors with intermediate fragility values as the glass transition is approached. Similar experiments using a high-purity  $[Bmim][BF_4]$  show that using a higher purity of the ionic liquid, while changing absolute values of the properties, does not eliminate the anomalous aging response. The data are also analyzed in a fashion similar to that used for polymer melts, and we find that these ionic liquids do not follow, for example, the Cox–Merz relationship between the steady shear viscosity and the dynamic viscosity.

## 1. Introduction

Ionic liquids are salts that are liquid at room temperature with melting points below 100 °C. They consist of organic cations and inorganic smaller anions.<sup>1,2</sup> Lately much attention has been drawn toward ionic liquids due to their unique properties, such as low vapor pressure, thermal stability, noncombustibility, electric conductivity and the ability to dissolve both organic and inorganic substances.<sup>3–6</sup> Ionic liquids do not crystallize readily and consequently are excellent candidates for the investigation of glass forming liquids.<sup>3</sup> It is well-known that, near to the glass transition temperature, the viscosity and relaxation time of the supercooled, glass forming system increase dramatically with the decrease of temperature.<sup>7,8</sup> One means of investigating the dynamics of such systems is through the measurement of the dynamic mechanical responses (viscoelastic moduli) as a function of temperature and frequency. A common, though not universal, observation in glass forming liquids is that these materials follow time–temperature superposition and the temperature dependence of relaxation time or viscosity is well approximated by the empirical Vogel–Fulcher–Tamman equation.<sup>8,9</sup> The fragility index obtained from the VFT equation is another important parameter that characterizes the structural behavior of such materials with respect to temperature.<sup>10</sup>

In addition to the dynamic measurements, it is useful to examine the steady state shear viscosity and its shear rate dependence. We have evaluated the well-known analogy between the linear and nonlinear viscoelastic property (the Cox–Merz rule<sup>11</sup>), which is often valid for molten polymers and entangled solutions<sup>12</sup> but not for complex or structured fluids,<sup>13</sup> for our series of ionic liquids.

The molecular aspects of ionic liquids have been intensively studied at room temperature by different spectroscopic methods, for example, optical Kerr effect<sup>14–17</sup> and nuclear magnetic

resonance spectroscopy.<sup>18–21</sup> Temperature dependent experiments using dielectric spectroscopy<sup>4</sup> and neutron scattering<sup>22,23</sup> have been conducted to investigate the dynamics of ionic liquids in both the supercooled liquid and glassy amorphous states. The general conclusions of these studies is that the structure of neat ionic liquids and their intermolecular interactions are complex and governed by Coulombic interactions, van der Waals forces, and hydrogen bonding interactions. Recently, molecular dynamics simulations have suggested the existence of a complex nanostructural morphology in pure ionic liquids.<sup>24–26</sup> However, many of the physical and structural properties near to the glass temperature are not fully characterized and it is of interest to investigate the dynamics of ionic liquids in the vicinity of the glass transition temperature.

In the present study, we determined the steady shear viscosity, the dynamic moduli  $G'$  and  $G''$ , and the dynamic viscosities of three ionic liquids of the imidazolium family, 1-butyl 3-methylimidazolium tetrafluoroborate ( $[Bmim][BF_4]$ ), 1-butyl 3-methylimidazolium hexafluorophosphate ( $[Bmim][PF_6]$ ), and 1-ethyl 3-methylimidazolium ethylsulfate ( $[Emim][EtSO_4]$ ), were investigated in a range of temperatures near to the glass temperature. We analyzed the results within the framework of the time–temperature superposition principle and find that the van Gurp and Palmen<sup>27</sup> plot provides a very good indicator for the quality of the time–temperature superposition in these systems. We also characterized the fragility of our ionic liquids from the temperature dependence of the shift factors or the viscosity. The effect of purity on dynamic responses of the  $[Bmim][BF_4]$  was also examined, and the results for a 99% pure sample, while different quantitatively from those obtained for the 97% pure material, are qualitatively similar.

An important result from the present investigation arises from an observation made in the context of establishing the limiting behaviors of the steady shear viscosity at low shear rates and the dynamic viscosity at low frequency. From linear viscoelasticity theory, these are identical. However, in our early experiments, as described subsequently, we found that the low frequency dynamic

\* To whom correspondence should be addressed. E-mail: greg.mckenna@ttu.edu.

**TABLE 1: Structure and Thermophysical Properties of the Ionic Liquids Investigated in This Work**

material	structure	molecular wt (g/mol)	T <sub>g</sub> (DSC) (°C)
97% [Bmim][BF <sub>4</sub> ]		226.02	-85.0
99% [Bmim][BF <sub>4</sub> ]			-85.5
[Bmim][PF <sub>6</sub> ]		284.18	-77.0
[Emim][EtSO <sub>4</sub> ]		236.29	-80.9

modulus was significantly higher than the zero shear rate viscosity. This apparent anomaly was resolved when we discovered that the ionic liquids studied, when cooled from a high temperature to the lower temperatures of interest, but still above the glass temperature, age in a way that the viscosity decreases. Importantly, to our knowledge there have not been prior reports of such anomalous aging at temperatures above the nominal glass transition temperature where the equilibration times should be on the order of <1 s but rather are on the order of hours. Further, the aging is accompanied by a softening (lower viscosity) rather than a hardening of the system, suggesting that at low temperatures the materials are becoming less ordered.

## 2. Experimental Methods

**2.1. Materials.** Three ionic liquids of the imidazolium family were investigated: [Bmim][BF<sub>4</sub>] (Sigma Aldrich, 97% purity), [Bmim][PF<sub>6</sub>] (Sigma Aldrich, 96% purity), and [Emim][EtSO<sub>4</sub>] (Sigma Aldrich, 95% purity). In order to examine effects of the ionic liquid purity on the results, we also investigated a higher purity [Bmim][BF<sub>4</sub>] material (EMD chemicals, 99% purity). The chemical structures and thermal properties are shown in Table 1. Two of the ionic liquids were chosen on the basis of their containing the same cation with the same alkyl chain length (butyl, [Bmim] derivatives), and one was chosen to have a shorter alkyl chain length (ethyl, [Emim]) cation. Each system had different anions. The change in alkyl chain length can cause changes in melting point and the tendency of the ionic liquid to form a glass rather than to crystallize on cooling. On the other hand, the thermal stability of ionic liquids depends strongly on the anions, and the general stability order is Cl<sup>-</sup> < [BF<sub>4</sub>]<sup>-</sup> ~ [PF<sub>6</sub>]<sup>-</sup>. Since a significant amount of moisture can be absorbed by ionic liquids at room temperature, it is important to keep the samples dry. Therefore, the ionic liquids were dried at 70 °C for 24 h under vacuum. Then they were sealed and stored in a desiccator. While in use, the ionic liquids were constantly under nitrogen environment to prevent moisture uptake from the atmosphere. The glass transition temperatures of the ionic liquids were measured by differential scanning calorimetry (DSC) by cooling the samples from 130 to -120 °C, followed by heating from -120 to 30 °C both at a rate of 10 °C/min. The DSC determined glass temperature reported is the fictive temperature.

**2.2. Rheological Measurements.** The rheological properties of the ionic liquids were measured using an advanced rheometric

expansion system (ARES, TA Instruments) strain controlled rheometer using both 8 and 25 mm diameter platens in a parallel plate geometry. The gap was monitored closely to keep a good sample shape by manually changing the gap with the change in temperature (the thermal expansion coefficient of the system is 2.516 μm/K). Steady shear and dynamic oscillatory shear experiments were carried out in the shear rate range of (1 × 10<sup>-5</sup>)–0.1 s<sup>-1</sup> and frequency range 0.001–100 rad/s, respectively. The mechanical responses of different ionic liquids were measured at temperatures from -70 to -87 °C, and the strain was varied between 0.1 and 1%. In the present paper, all the dynamic data presented are compliance corrected using the correction method reported by Hutcheson and McKenna.<sup>8</sup> The compliance of the total system using 4 and 12.5 mm radius platens is 8.102 × 10<sup>-3</sup> and 6.923 × 10<sup>-3</sup> rad/Nm respectively.<sup>8</sup>

During the current study we used a custom designed strain-gage transducer, which is more robust than the 2K FRT (Force Rebalanced) transducer provided by the instrument manufacturer. It has a torque range of 8500 g cm and normal force range of 5000 g. Most of the experiments were carried out in the 8 mm parallel plate geometry. However, the increase in temperature above T<sub>g</sub> decreases the torque dramatically, which leads to error in the dynamic results. Therefore, experiments performed at the higher temperatures were carried out in the 25 mm parallel plate geometry. To control the experimental temperature far below room temperature, liquid nitrogen was used as the coolant. This also had the effect of providing a nitrogen blanket to protect the sample from moisture absorption. The ARES system uses a PID temperature controller to control the temperature, and it was measured by the oven PRT. The temperature varied by ±0.5 °C relative to the set temperature.

**2.3. Aging Tests.** As mentioned in the Introduction, we found that the material ages at temperatures near to but above the glass temperature. Without prior knowledge of the nature of the aging, we chose to perform the aging experiments in a protocol similar to that developed by Struik<sup>28</sup> for samples aged below the glass transition temperature, but adapted to the conditions of examining both steady shear response and the dynamic viscosity for the materials. The aging experiments included both small amplitude oscillatory shear (dynamic frequency sweep) and steady shear deformation measurements at different aging times. For these tests the sample was first kept at room temperature for 30 min and then quenched to the temperatures of interest (near T<sub>g</sub>), where we found the aging to be important. It was suggested by Struik's<sup>28</sup> protocol that the aging time should be 10 times higher than the duration of the load application time to minimize the effects of previous structural recovery, and our experiments were performed to respect this requirement. Furthermore, the aging time between sequential experiments at a given temperature was approximately 10 times the duration of the mechanical test being performed.

## 3. Results and Discussion

**3.1. Dynamic Data.** Figure 1a–c shows the results of measurements of the dynamic storage and loss moduli for [Bmim][BF<sub>4</sub>] for the temperature range from -87 to -77 °C. Figure 1a,b shows that the low frequency ends of both G' and G'' show the typical limits of proportionality to frequency as ω<sup>2</sup> and ω, as expected.<sup>12</sup> Due to the torque limitations of the torque transducer in the low frequency range, rheological data at much lower frequencies could not be obtained, though the observation of limiting terminal behavior suggests that any further relaxations are unlikely. The range of temperatures was somewhat extended using the largest available plated diameter

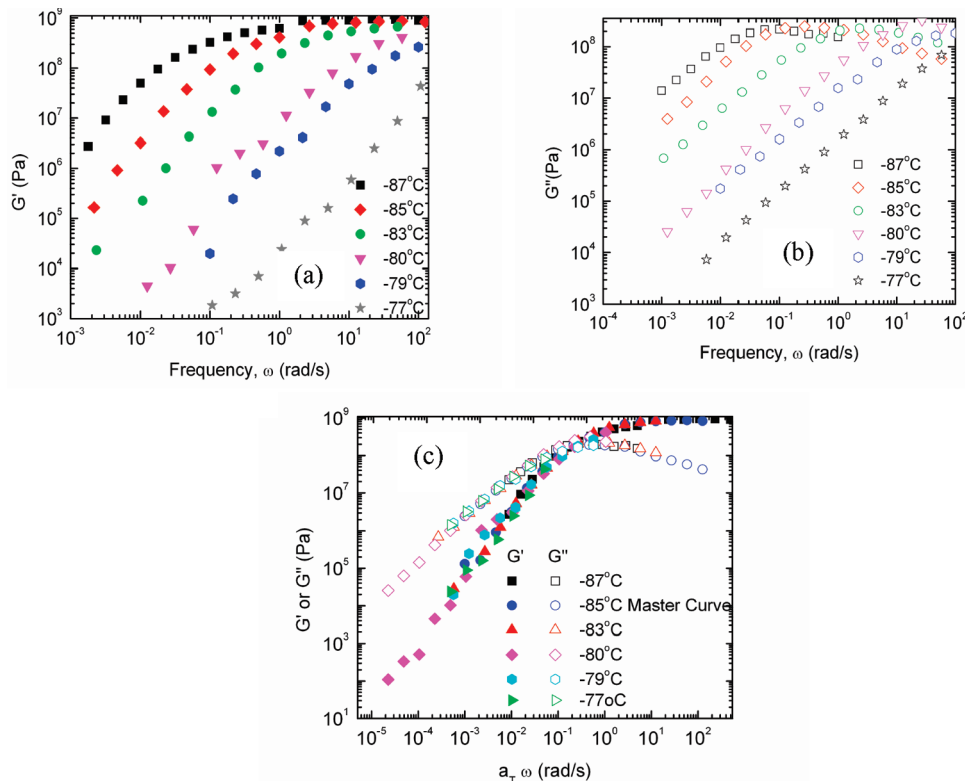


**Figure 1.** Double logarithmic representation of (a) storage and (b) loss modulus vs angular frequency for  $[\text{Bmim}][\text{BF}_4]$  at temperatures from  $-87$  to  $-77$   $^{\circ}\text{C}$ . (c) Master curve representation of storage and loss moduli vs reduced frequency  $a_T \omega$ .

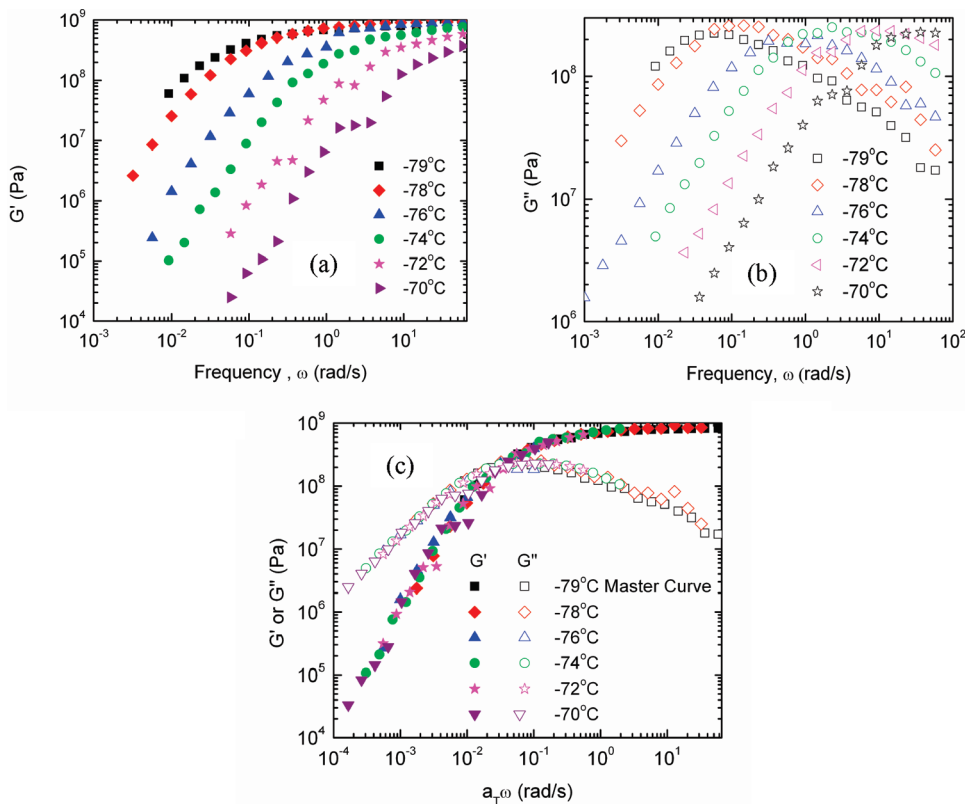


**Figure 2.** Double logarithmic representation of (a) storage and (b) loss modulus vs angular frequency for  $[\text{Bmim}][\text{PF}_6]$  at temperatures from  $-79$  to  $-70$   $^{\circ}\text{C}$ . (c) Master curve representation of storage and loss moduli vs reduced frequency  $a_T \omega$ .

of 25 mm for said measurements, e.g.,  $-77$   $^{\circ}\text{C}$  for  $[\text{Bmim}][\text{BF}_4]$ . Figure 1c shows the master curve of  $G'$  and  $G''$  vs  $a_T \omega$  created using time-temperature superposition to superimpose the data

of Figure 1a,b. Figures 2a–c and 3a–c show that a similar response behavior and time-temperature superposition behavior were attained for  $[\text{Bmim}][\text{PF}_6]$  and  $[\text{Emim}][\text{EtSO}_4]$ . We remark

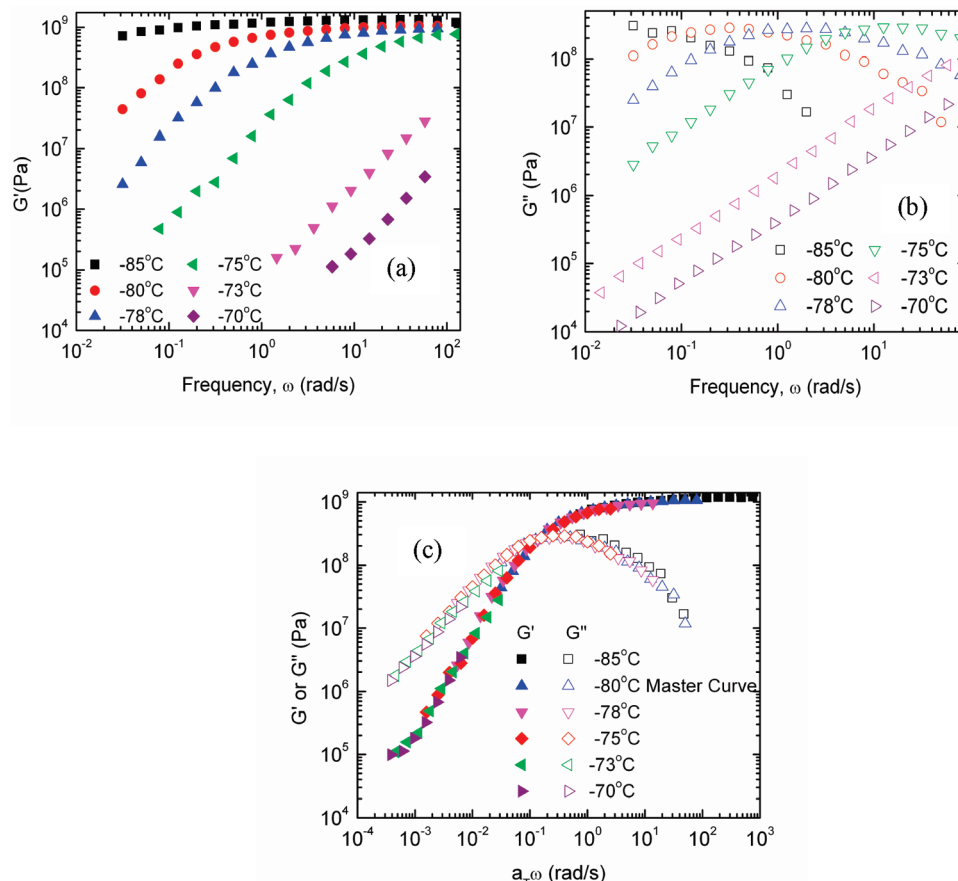


**Figure 3.** Double logarithmic representation of (a) storage and (b) loss modulus vs angular frequency for  $[\text{Emim}][\text{EtSO}_4]$  at temperatures from  $-85$  to  $-70$   $^{\circ}\text{C}$ . (c) Master curve representation of storage and loss moduli vs reduced frequency  $a_T \omega$ .

that, because of the aging behavior described subsequently, the results presented in Figures 1–3 were carried out at the equilibrium condition after aging had ceased.

**3.2. Steady Shear vs Dynamic Viscosities: The Cox–Merz Rule.** A common manner of treating and comparing dynamic viscosity data with steady shear data is the empirical Cox–Merz rule.<sup>11,12</sup> In the limit of zero frequency and zero shear rate, of course, the dynamic viscosity  $\eta^*$  and the zero shear viscosity  $\eta_0$  should be the same. The shear rate and frequency dependences coincide only when the Cox–Merz rule is followed, which is often the case for entangled polymeric melts in the terminal flow regime.<sup>29,30</sup> Figure 4 presents plots of  $\log \eta^*$  and  $\log \eta_0$  vs  $\log \omega$  or  $\log \dot{\gamma}$ , respectively, for the  $[\text{Bmim}][\text{BF}_4]$  and the  $[\text{Bmim}][\text{PF}_6]$  liquids. We see that the behavior deviates from the Cox–Merz<sup>11</sup> rule in that the zero shear viscosity  $\eta_0$  begins to show shear thinning behavior at  $\dot{\gamma}$  values that are smaller than the values of  $\omega$  at which the dynamic viscosity begins to show a decrease with frequency. This is in contrast to the general behavior of polymeric fluids in the entanglement regime.<sup>31,32</sup> It is not unexpected because the glassy dispersion is fundamentally different from the entanglement or terminal dispersion of polymer melts. The Cox–Merz rule is also known to fail for entangled polymeric fluids, which exhibit strong energetic interactions like hydrogen bonds or clustered ionomers,<sup>33,34</sup> as well as for branched polymers.<sup>35,36</sup> In fact, in our view, the thought that the Cox–Merz rule “is a suspicious coincidence” is the most pertinent and there is no fundamental reason that it should work, as relating linear to nonlinear properties is not straightforward.<sup>12,36,37</sup>

**3.3. Temperature Dependences.** The temperature dependences of the shift factors used to create the master curves of

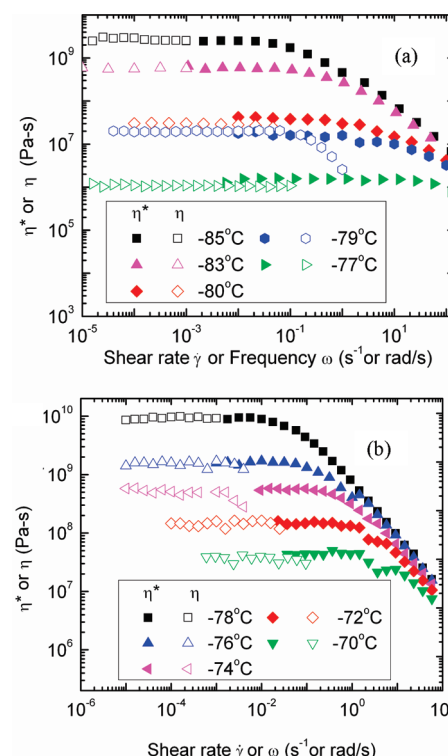


**Figure 4.** Double logarithmic plot of the steady state (open symbol) and the complex (closed symbol) viscosity of (a)  $[\text{Bmim}][\text{BF}_4]$  within a temperature range from  $-85$  to  $-77$   $^{\circ}\text{C}$ , and (b)  $[\text{Bmim}][\text{PF}_6]$  within a temperature range from  $-78$  to  $-70$   $^{\circ}\text{C}$  as a function of  $\dot{\gamma}$  and  $\omega$ , respectively.

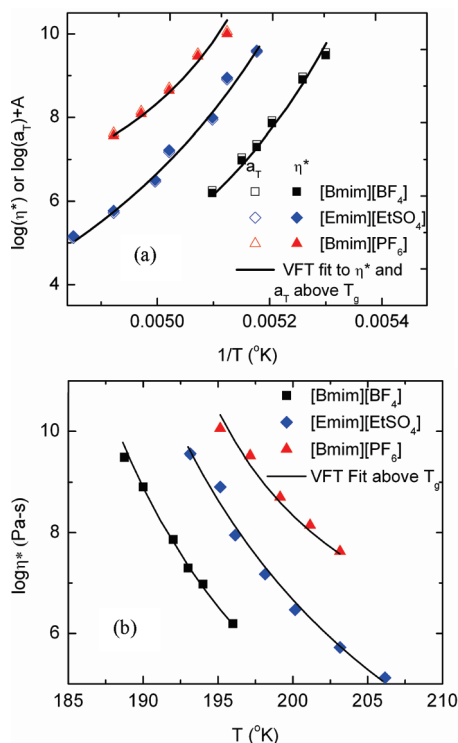


**Figure 5.** Dynamic viscosity (closed symbols) and time–temperature shift factor (open symbols) for three ionic liquids vs (a) reciprocal temperature and (b) temperature. The shift factors are vertically shifted by a factor  $A$  to coincide with the viscosity. The black solid line is the VFT fit to the dynamic viscosity and shift factor at  $T_g$  and above  $T_g$ .

Figures 1c, 2c, and 3c and the dynamic viscosities at low frequency are presented for the three ionic liquids in Figure 5a,b. The shift factor  $a_T$  is evaluated as the ratio of  $\eta(T)/\eta(T_{\text{ref}})$  ( $\eta = \eta^*$  at the limiting frequency), where the reference temperature is the reference temperature of the dynamic data master curve and the temperature dependence of the viscosities is well described by the Vogel–Fulcher–Tamman Equation.<sup>38–40</sup> The shift factors were shifted by a factor  $A = 9.5$  and are, then, in agreement with the dynamic viscosity data. The VFT equation is given as follows:<sup>38–40</sup>

$$\eta(T) = \eta_0 \exp\left(\frac{B}{T - T_g}\right)$$

or

$$\tau(T) = \tau_0 \exp\left(\frac{B}{T - T_g}\right) \quad (1)$$

where  $\eta_0$  and  $\tau_0$  are infinite high-temperature viscosity and relaxation time (or simply prefactors), respectively.  $T_\infty$  is the VFT divergence temperature and  $B$  is a material specific parameter. When the viscosity vs inverse of temperature shows almost Arrhenius-like behavior, the liquids are known as strong liquids, whereas strongly convex curves are considered as fragile.<sup>41</sup> Therefore, the dynamic fragility can be written in terms of VFT parameters.<sup>38–40</sup> The VFT parameters related to dynamic fragility  $m$  and apparent activation energy  $E_g$  at  $T_g$  are as follows:<sup>42,43</sup>

$$m = \frac{B/T_g}{\ln 10(1 - T_\infty/T_g)^2} \quad (2)$$

$$E_g = \frac{RB}{(1 - T_\infty/T_g)^2} \quad (3)$$

The ionic liquids investigated here are good glass formers, and fragility is one of the central phenomena of glassy state physics that reflects the stability of the liquid structure to thermal degradation.<sup>44</sup> The dynamic fragility and apparent activation energy at  $T_g$  for the three ionic liquids are presented in Table 2. The results show that these ionic liquids have similar dynamic fragility values (between  $m = 73$  and 80) despite the fact that they have different anions. The (apparent) activation energy of the ionic liquids at  $T_g$  is in the range of 200–350  $\text{kJ mol}^{-1}$ , which is similar to the activation energy of other types of ionic glass formers reported by other researchers,<sup>43,45</sup> except the BMI-BOB high fragility ionic liquid that shows higher activation energy.<sup>46</sup> According to the investigation of Qin and McKenna<sup>43</sup> on different classes of glass forming liquids, the effect of  $T_g$  on the fragility of inorganic glasses is insignificant and the dynamic fragility fall in a range of 16–55 over a fairly wide range of  $T_g$ . Therefore, we conclude that the fragility of the ionic liquids studied here falls in the intermediate region and the dynamic fragility of the three ILs is relatively insensitive to alkyl chain length ( $m_{\text{BF}_4} = 79$ ,  $m_{\text{EtSO}_4} = 80$ ,  $m_{\text{PF}_6} = 73$ ). Similarly, Leys et al.<sup>47</sup> extensively studied the dependence of the VFT curves on the alkyl chain length of the homologous series of 1-alkyl 3-methylimidazolium tetrafluoroborate ( $[\text{C}_n\text{mim}]\text{[BF}_4]$ , where  $n = 2–11$ ) and concluded that fragility is only weakly dependent on alkyl chain length. They explained that fragility of ionic liquids strongly depends on the local interionic Coulombic forces that are between the anion and the imidazolium part of the cation and thus only indirectly influenced by alkyl chain length. Moreover, Xu and Angell<sup>48</sup> compared the fragility of ionic liquids with liquids of other type and reported that the fragility of ionic liquids varies from intermediate to extremely fragile, depending on the anion. In addition to being subject to cation and anion effects, the fragility index of ionic liquids also depends on the choice of  $T_g$ .<sup>48</sup> In the present study, we used the  $T_g$  defined as that corresponding to a 100 s relaxation time calculated from the VFT fit to the relaxation time over a range of temperatures (data not shown here). It is observed that the 100 s  $T_g$  so obtained is slightly lower than the glass transition temperature obtained by differential scanning calorimetry (compare Tables 1 and 2).

**3.4. van Gurp–Palmen Analysis.** A sensitive measure of the validity of time–temperature superposition and to determine the modulus of a material is the van Gurp–Palmen plot<sup>49,50</sup> (or simply the van Gurp plot), which depicts the phase angle  $\delta$  vs the corresponding absolute value of the complex shear modulus obtained from the dynamic rheological data. In the case of the rubbery plateau modulus of an entangled polymer, the van Gurp–Palmen plot gives  $G^\infty = \lim_{\delta \rightarrow 0} |G^*(\delta)|$ .<sup>51</sup> Here we examine the dynamic responses of the ionic liquids within this

**TABLE 2: Dynamic Fragility and Apparent Activation Energy at  $T_g$  for the Three Ionic Liquids Investigated**

ionic liquids	$T_\infty$ ( $^{\circ}\text{C}$ )	$T_g$ (100 s) ( $^{\circ}\text{C}$ )	$m$	$E_g$ (kJ/mol)
[Bmim][BF <sub>4</sub> ] (97%)	$-101.1 \pm 1.7$	-87	79	280
[Bmim][PF <sub>6</sub> ]	$-89.6 \pm 1.5$	-79	73	231
[Emim][EtSO <sub>4</sub> ]	$-101.6 \pm 1.2$	-86	80	316

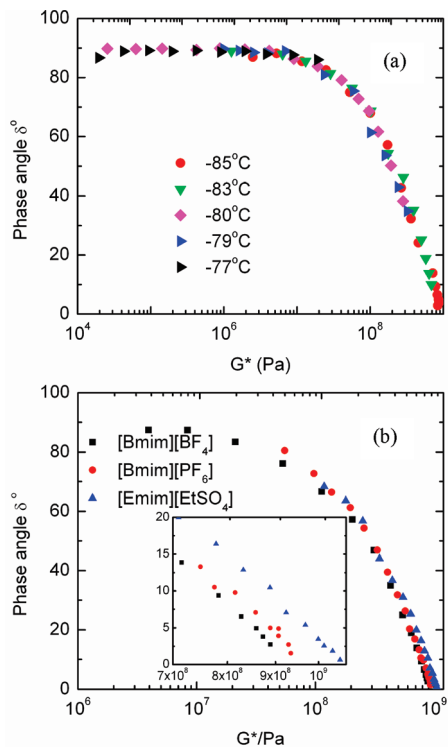


**Figure 6.** (a) The van Gurp–Palmen plot for  $[\text{Bmim}][\text{BF}_4]$  at different temperatures and (b) the van Gurp–Palmen plot for the three ionic liquids at their respective  $T_g$  values.

context. Figure 6a shows a van Gurp–Palmen plot for  $[\text{Bmim}][\text{BF}_4]$  at different temperatures. In the plot, the value of  $G^*$  as  $\delta \rightarrow 0^\circ$  scatters around  $1 \times 10^9$  Pa for the ionic liquids and this corresponds to the glassy modulus. One sees also in Figure 6a that the time–temperature superposition is well satisfied, as the data at different temperatures fall on a single curve. Similar behavior was observed for the other liquids. Thus, our result is consistent with the master curve generated using the time–temperature superposition of the previous dynamic results. Figure 6b shows the van Gurp–Palmen plots for the three ionic liquids at each material’s glass transition temperature (DSC). We see in the inset that there is a slight dependence of the glassy modulus  $G^*(\delta=0^\circ)$  on the ionic liquid structure.

**3.5. Anomalous Aging Behavior.** As indicated in the Introduction, the above discussion refers to data obtained on

materials in equilibrium. However, in the work we carried out to obtain that data, we found an anomalous aging behavior in these ionic liquids that occurred above the glass transition temperature and that, to our knowledge, has not been previously observed in ionic or other glass forming liquids in this regime. The finding of the aging effects came about because we compared the zero shear rate viscosity with the dynamic viscosity in our earliest tests on these ionic liquids. There, following a procedure in which we performed the dynamic tests before the steady shear tests, we found the anomaly that the low frequency dynamic viscosity was greater than the zero shear rate (steady state) viscosity.

In those early tests, we used the following procedure: at first the samples were kept at room temperature for 15 min and then rapidly cooled (quenched) to the temperature of interest (near  $T_g$ ), where the sample was held for another 30 min for the temperature to stabilize. We then performed the dynamic frequency sweep to obtain the dynamic moduli and dynamic viscosity. The dynamic frequency sweep tests took about 7–8 h to complete in the direction of decreasing frequency (approximately 100–0.001 rad/s). Following the frequency sweep test at the relevant temperature, we performed the steady shear experiments. However, because of the time involved in performing a typical frequency sweep, the samples were effectively “aged” prior to the steady shear experiments. Typical results for the dynamic viscosity and the steady state viscosity under these test conditions are shown in Figure 7, and we see the anomalous differences in  $\eta_0$  and  $\eta^*$  at the low frequency or shear rate. Perhaps more interesting is that the dynamic viscosity increases through a maximum in these experiments. We remark that, as temperature increases, the steady state viscosity at low shear rates becomes equal to the dynamic viscosity and the maximum with frequency in the dynamic viscosity disappears. To try to establish the origins of this anomalous discrepancy between zero shear rate and zero frequency viscosities (recall this is a requirement of linear viscoelasticity) for the ionic liquids, we conducted the second dynamic frequency sweep (DFS) test after the first one for  $[\text{Bmim}][\text{BF}_4]$  and  $[\text{Bmim}][\text{PF}_6]$ ; i.e., we had effectively aged the sample. The results are also included in Figure 7, and it can be seen that for the aged material the dynamic viscosity has decreased and  $\eta^*$  matches  $\eta_0$  at the limiting values, i.e.  $\lim_{\dot{\gamma} \rightarrow 0} \eta(\dot{\gamma}) = \lim_{\omega \rightarrow 0} \eta^*(\omega)$ .

To further explore the origins of the anomalous differences in the steady state and dynamic viscosities of our ionic liquids, we investigated in some detail the aging behavior of  $[\text{Bmim}]$

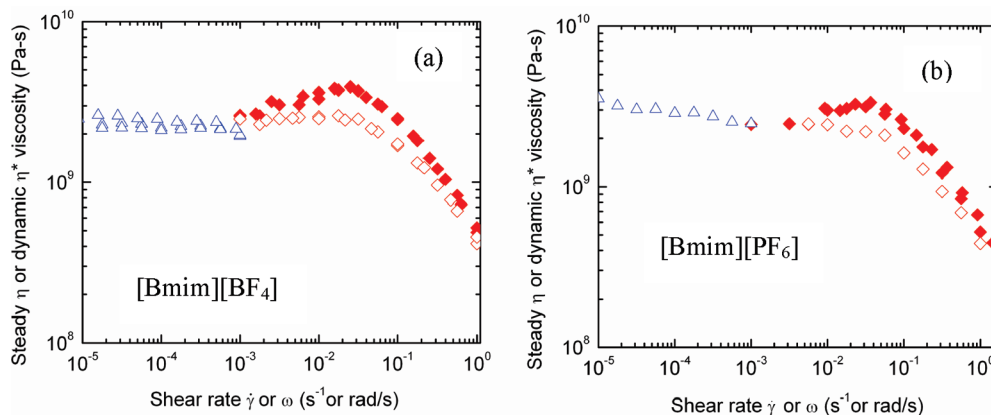


**Figure 7.** The repeated tests of dynamic viscosity (red diamond) and the steady state viscosity (blue triangle) of ionic liquids  $[\text{Bmim}][\text{BF}_4]$  (a) and  $[\text{Bmim}][\text{PF}_6]$  (b). The dynamic tests (closed symbols) were conducted immediately after sample input, while the open symbols represent tests that were conducted after the first dynamic test. The steady state (open triangles) viscosity tests were carried out after each dynamic test in the equilibrium state.

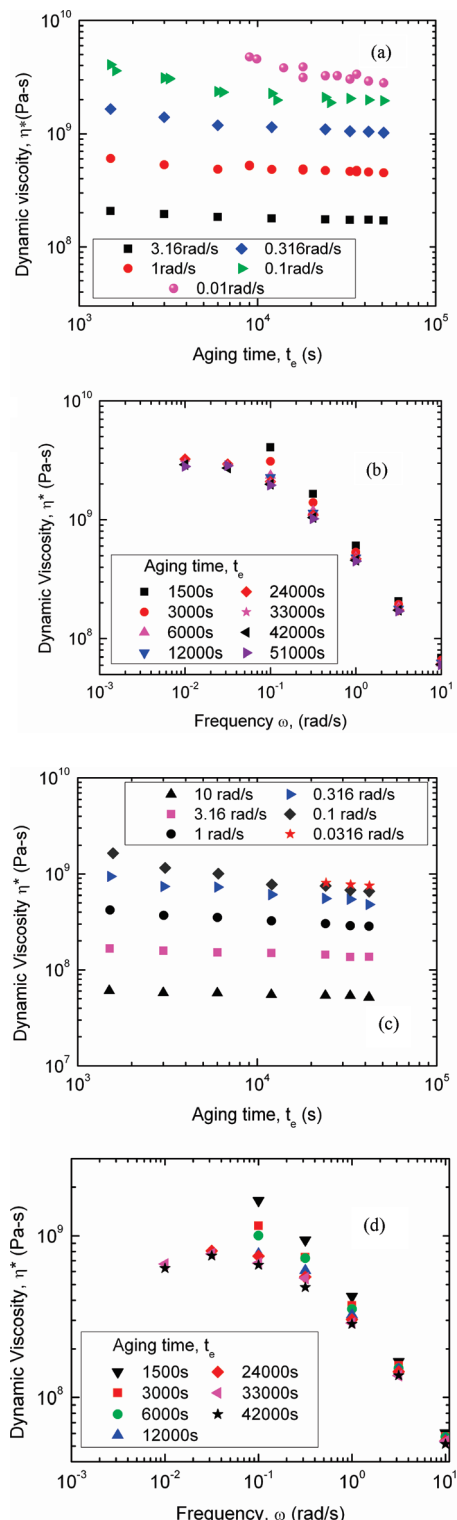


**Figure 8.** Double logarithmic representation of dynamic viscosity vs aging time ( $t_e$ ) and frequency for  $[\text{Bmim}][\text{BF}_4]$  at  $-85\text{ }^\circ\text{C}$  (a, b) and  $-83\text{ }^\circ\text{C}$  (c, d).

$[\text{BF}_4]$  near to but above its glass transition temperature. The aging responses for  $[\text{Bmim}][\text{BF}_4]$  at  $-85$  and  $-83\text{ }^\circ\text{C}$  are shown in Figure 8a–d. We chose five or six frequencies at each temperature and carried out the dynamic frequency sweep at the given aging times. The dynamic viscosity vs the aging time at different frequencies for  $-85$  and  $-83\text{ }^\circ\text{C}$  are presented in parts a and c of Figure 8, respectively. In addition and to clearly show the interesting increase of dynamic viscosity through a

maximum, we present the dynamic viscosity as a function of frequency at different aging times in Figure 8b,d for the same temperatures. Since we followed Struik's protocol for the aging experiments, the ratio of the mechanical test duration to the increasing aging times was constant at 0.1. As a result, we did not obtain the dynamic viscosity at lower frequencies for the shortest aging times.

We note that at the lowest and highest frequencies, the change of dynamic viscosity with aging time is not very pronounced. However, at the intermediate frequencies, we see a significant decrease of the viscosity with increasing aging time at both  $-85$  and  $-83\text{ }^\circ\text{C}$ . This behavior is consistent with our previous finding (Figure 7), where we observed that as the temperature increases the maximum in the dynamic viscosity with frequency disappears and the low frequency dynamic viscosity becomes equal to steady shear rate viscosity. Figure 8b,d clearly shows the maximum in the dynamic viscosity and that, with increasing aging time, it gradually diminishes.

Since the dynamic viscosity of the ionic liquid  $[\text{Bmim}][\text{BF}_4]$  shows frequency dependent aging, we also investigated the aging response of the steady state viscosity. We carried out shear rate sweeps at different aging times. The sweeps were performed sequentially at the given aging time and used four rates from  $1 \times 10^{-5}$  to  $1 \times 10^{-3}\text{ s}^{-1}$  at the different aging times. Higher shear rates were not used, as the samples fractured under these conditions. Figure 9a–d shows the double logarithmic representations of steady state viscosity vs shear rate and aging time for  $[\text{Bmim}][\text{BF}_4]$  at  $-85$  and  $-83\text{ }^\circ\text{C}$ . From the figure we see that the viscosity decreases as aging time increases. Figure 9a,b shows that the material did not reach equilibrium after 9 h of aging for the shear rate sweep data at  $-85\text{ }^\circ\text{C}$ . On the other hand, the steady state viscosity reported in Figure 4a for the  $[\text{Bmim}][\text{BF}_4]$  at  $-85\text{ }^\circ\text{C}$  are for equilibrium, but after only 8 h of aging, that occurs during a dynamic frequency sweep test. It seems that the dynamic oscillation accelerates the aging so that the material reaches equilibrium more quickly in the oscillatory frequency sweep experiments than in the shear rate sweep aging experiments. Since we followed Struik's protocol for the aging experiments, we did not obtain data for the shear rate sweep for aging times longer than 9 h, as the liquid nitrogen capacity available to us was insufficient to investigate longer aging times and still be consistent with the protocol. It is interesting to remark that the relationship between the viscosity and the aging time is opposite to that observed during aging in the glassy state; i.e., here we see the viscosity (or equivalently relaxation time) decreasing as aging time increases, while generally glassy aging is accompanied by increases in viscosity or relaxation time.<sup>10,28</sup> Comparing the results for the two temperatures we observe that the  $[\text{Bmim}][\text{BF}_4]$  reaches equilibrium more quickly at  $-83\text{ }^\circ\text{C}$ .

**3.6. High-Purity  $[\text{Bmim}][\text{BF}_4]$  (99%).** Ionic liquids are highly complex solvents. It is difficult to purify ionic liquids by traditional crystallization and distillation techniques because of their low freezing points and negligible vapor pressures.<sup>52</sup> In 1992, Wilkes and Zaworotko<sup>53</sup> reported air and moisture insensitive ionic liquids based on 1-ethyl-3-methylimidazolium cation with either tetrafluoroborate or hexafluorophosphate as anions. However, the exposure of these materials to moisture for a long time can cause some changes in their physical and chemical properties.<sup>54</sup> Recently, Endres<sup>55</sup> in his editorial discussed that "slight changes in the ionic structure or in the purity can influence the physicochemical reactions of ionic liquids". In the present section we compare the rheological results obtained for a high-purity (99%)  $[\text{Bmim}][\text{BF}_4]$  with those for the 97% pure  $[\text{Bmim}][\text{BF}_4]$  reported above.

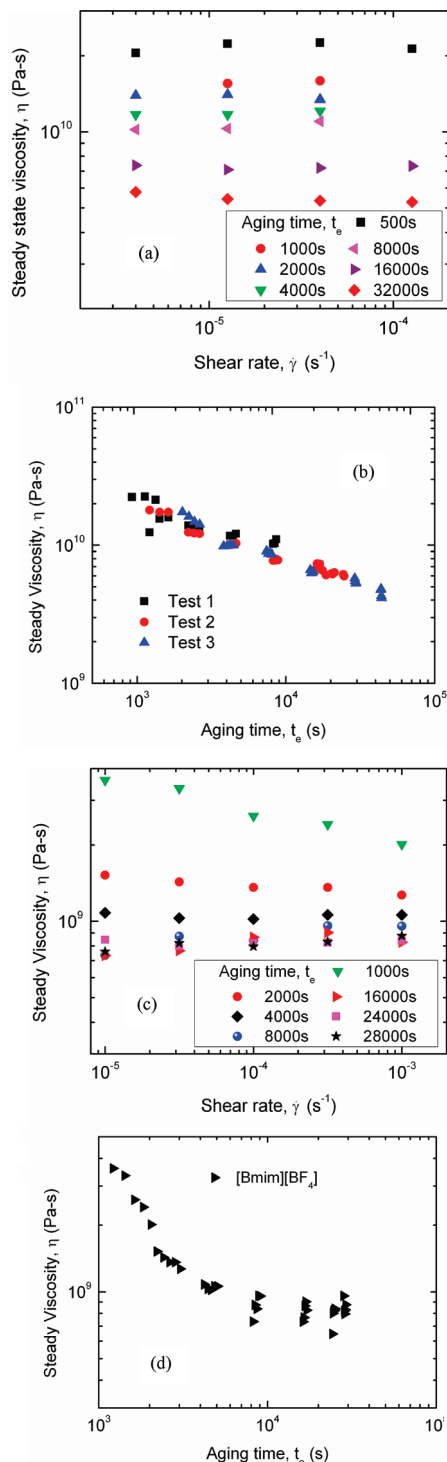


**Figure 9.** Double logarithmic representation of steady state viscosity vs shear rate and aging time ( $t_e$ ) of [Bmim][BF<sub>4</sub>] at  $-85^\circ\text{C}$  (a, b) and  $-83^\circ\text{C}$  (c, d).

**3.7. General Purity Issues.** The storage and loss moduli of high-purity [Bmim][BF<sub>4</sub>] at a temperature range from  $-87$  to  $-77^\circ\text{C}$  are shown in Figure 10a,b. The results show similar dynamic response behavior to the 97% pure [Bmim][BF<sub>4</sub>]. In both cases,  $G'$  and  $G''$  decrease and are approximately proportional to  $\omega^2$  and  $\omega$  in the terminal frequency regime. Figure 10c shows the master curves for  $G'$  and  $G''$  vs  $a_T\omega$  created using time–temperature superposition to superimpose the data of Figure 10a,b. Since highly pure [Bmim][BF<sub>4</sub>] also showed

anomalous aging behavior, the results presented in Figure 10 were carried out at the equilibrium condition.

**3.8. Anomalous Aging of the High-Purity Material.** Similar to the anomalous aging behavior of 97% pure [Bmim][BF<sub>4</sub>], we also found the aging anomaly for the 99% pure [Bmim][BF<sub>4</sub>] that the low frequency dynamic viscosity was greater than the zero shear rate (steady state) viscosity. We followed the same test sequence used for the 97% pure ionic liquid (see previous description) to age the higher purity ionic liquid. The results for the dynamic viscosity and the steady state viscosity under these test conditions are shown in Figure 11. It can be seen that for the aged material the dynamic viscosity has decreased and  $\eta^*$  matches  $\eta_0$  at the limiting values; i.e.,  $\lim_{\dot{\gamma} \rightarrow 0} \eta(\dot{\gamma}) = \lim_{\omega \rightarrow 0} \eta^*(\omega)$ .

**3.9. Viscosity Behavior of High-Purity [Bmim][BF<sub>4</sub>].** The plot of  $\log \eta^*$  and  $\log \eta_0$  vs  $\log \omega$  or  $\log \dot{\gamma}$  for the high-purity [Bmim][BF<sub>4</sub>] is shown in Figure 12. It was found that the viscosity decreases with increasing temperature and the highly pure [Bmim][BF<sub>4</sub>] also does not follow the Cox–Merz<sup>11</sup> rule of melt rheology. Similar to the 97% pure [Bmim][BF<sub>4</sub>], the 99% purity ionic liquid shows shear thinning behavior at a lower shear rate than the frequency. However, we observed differences in the low frequency or zero shear rate viscosity of highly pure [Bmim][BF<sub>4</sub>] from those of the 97% pure [Bmim][BF<sub>4</sub>]. The viscosity is slightly higher for the 99% pure [Bmim][BF<sub>4</sub>] compared with the 97% material at high temperatures, and the viscosities approach each other near to their common  $T_g$ . The observed increase in viscosity may be due to stronger van der Waals forces between cations and also the ability of anions to form hydrogen bonds.<sup>56</sup> This is seen in Figure 13, where the viscosities of the 97% material are reproduced along with those of the 99% [Bmim][BF<sub>4</sub>].

The temperature dependence of the dynamic viscosity is non-Arrhenius and fits well to the Vogel–Fulcher–Tammann law<sup>38–40</sup> (eq 1), which is conventional for typical glass formers. The shift factors from the dynamic moduli were shifted by a factor  $A = 9.5$  and are, then, in agreement with the dynamic viscosity data. The fragility and activation energy of the 99% [Bmim][BF<sub>4</sub>] were calculated using eqs 2 and 3, respectively. The dynamic fragility of the 99% [Bmim][BF<sub>4</sub>] is 63 and the activation energy is 225 kJ mol<sup>-1</sup>, which are lower than the fragility and activation energy of the 97% pure [Bmim][BF<sub>4</sub>] (Table 2). The fragility index was calculated using the glass transition temperature defined as the temperature at which the relaxation time is 100 s; i.e.,  $T_g = -87^\circ\text{C}$ .

To examine the validity of time–temperature superposition and the modulus of the material, we studied the Van Gurp–Palmen<sup>49</sup> plot. Figure 14 shows a van Gurp–Palmen plot for the 99% [Bmim][BF<sub>4</sub>] at different temperatures. In the plot, the value of  $G^*$  as  $\delta \rightarrow 0^\circ$  scatters around  $1 \times 10^9$  Pa for the ionic liquid and this corresponds to the glassy modulus. Also the time–temperature superposition is well satisfied, as the data at different temperatures fall on a single curve. Similar behavior was observed for the 97% pure ionic liquid.

At the present time, we do not have an explanation for the anomalous aging of the ionic liquids. It seems that a possible reason for the observed softening of the materials with aging time is related to nanostructures in the ionic liquids, but why these would “disappear” during aging after a quench from a higher temperature is unclear. Certainly, the molecular organization of ionic liquids is different from traditional complex fluids, and researchers have reported that they can be nanostructured.<sup>57,58</sup> For example, Triolo et al.<sup>58,59</sup> used X-ray diffraction to show the existence of nanoscale segregation in the pure imidazolium

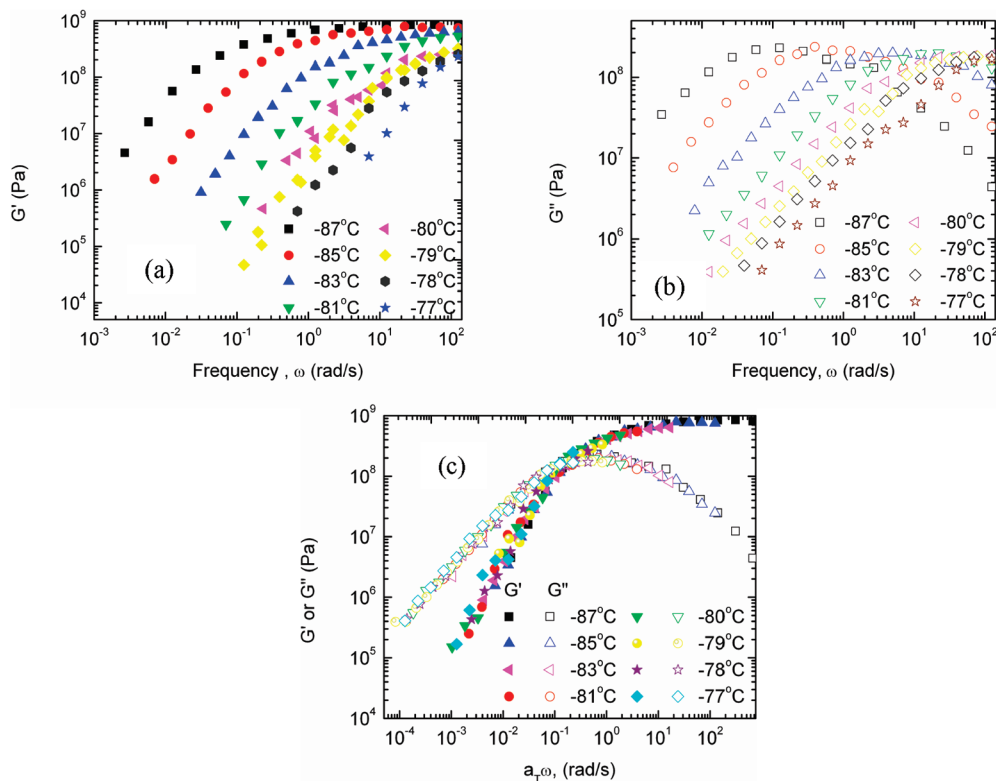


**Figure 10.** Double logarithmic representation of (a) storage and (b) loss modulus vs angular frequency for high-purity  $[Bmim][BF_4]$  at temperatures from  $-87$  to  $-77$   $^{\circ}C$ . (c) Master curve representation (at  $-85$   $^{\circ}C$ ) of storage and loss moduli vs reduced frequency  $a_T\omega$ .

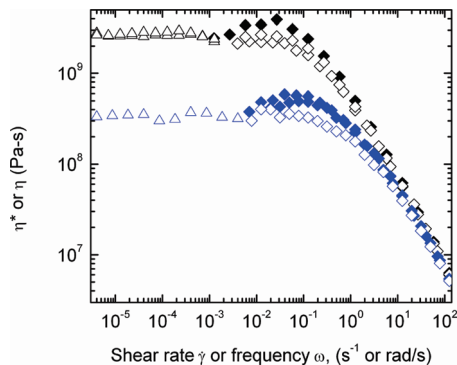


**Figure 11.** The repeated tests of dynamic viscosity at  $-85$   $^{\circ}C$  (black diamond) and  $-83$   $^{\circ}C$  (blue diamond) and the steady state viscosity (black and blue triangles) at  $-85$  and  $-83$   $^{\circ}C$ , respectively, of high-purity  $[Bmim][BF_4]$ . The closed symbol of the dynamic tests was conducted immediately after sample input, while the open symbol tests were conducted after the first dynamic test. The steady state (open triangles) viscosity tests were carried out after each dynamic test in the equilibrium state.

based ionic liquid at both room temperature and in the supercooled state. In the present study, we did not carry out any structural investigation of the materials, and these would seem to be appropriate experiments to undertake in future investigations.

#### 4. Summary

The dynamics of three imidazolium based ionic liquids near to but above their glass temperatures was studied using mechanical spectroscopy. This is the first investigation of the dynamic and steady state properties of  $[Bmim][BF_4]$ ,  $[Bmim][PF_6]$ , and  $[Emim][EtSO_4]$  near their respective glass transition

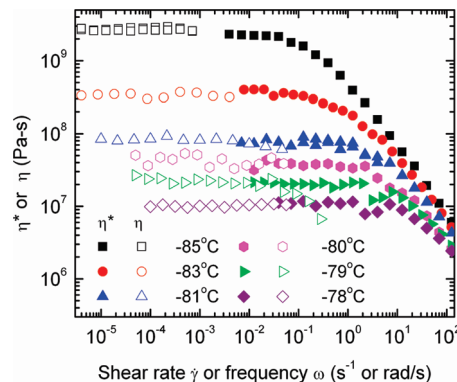


**Figure 12.** Double logarithmic plot of the steady state (open symbol) and the complex (closed symbol) viscosity of high-purity  $[Bmim][BF_4]$  within a temperature range from  $-87$  to  $-78$   $^{\circ}C$  as a function of  $\dot{\gamma}$  and  $\omega$ , respectively.

temperatures. The results indicate that these ionic liquids are good glass formers and that their equilibrium responses above the glass temperature follow time-temperature superposition, as indicated by direct superposition of the data and by a van Gurp-Palmen<sup>49</sup> analysis. The steady shear rate viscosity  $\eta(\dot{\gamma})$ , compared to the dynamic complex viscosity  $\eta^*(\omega)$ , of these ionic liquids does not follow the conventional melt rheology of liquids, such as the Cox-Merz rule. In the linear viscoelastic response region, the temperature dependence of viscosity and shape factor is non-Arrhenius but fits well to the Vogel-Fulcher-Tamman (VFT) equation. The fragility index estimated by using the VFT equation shows that these ionic liquids fall in the intermediate region of fragility index ( $m \approx 73-80$ ) and they are relatively insensitive to the alkyl chain length.

We discovered that there is an anomalous aging response in these liquids and performed an extensive investigation of aging

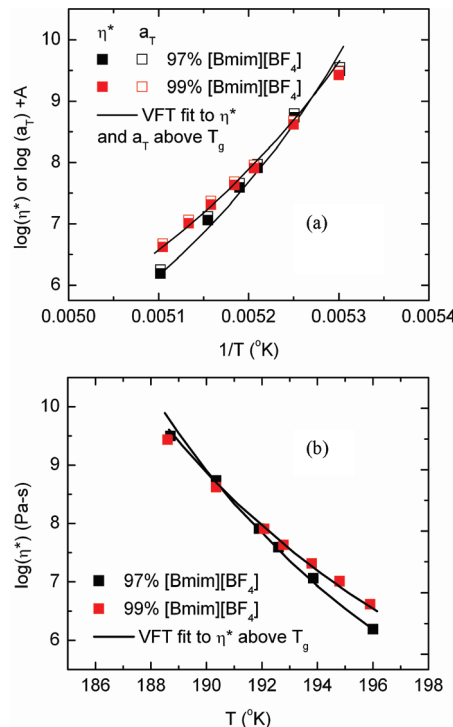


**Figure 13.** Dynamic viscosity (closed symbols) and time-temperature shift factor (open symbols) for high-purity 99% (red squares) and 97% [Bmim][BF<sub>4</sub>] (black squares) vs (a) reciprocal temperature and (b) temperature. The shift factors are vertically shifted by a factor  $A$  to coincide with the viscosity. The black solid line is the VFT fit to the dynamic viscosity and shift factor at  $T_g$  and above  $T_g$ .

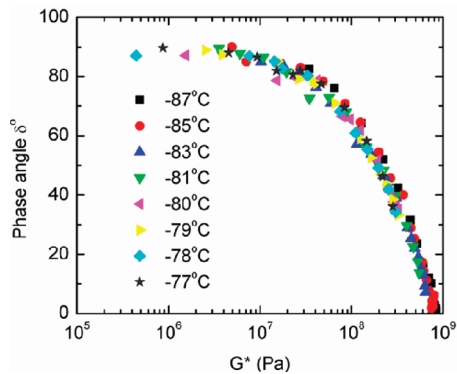


**Figure 14.** The van Gurp-Palmen plot for high-purity [Bmim][BF<sub>4</sub>] at different temperatures.

both of the dynamic and steady state viscosities for [Bmim]-[BF<sub>4</sub>]. Surprisingly, the viscosity of the liquid decreases with increasing aging time, unlike aging in the glassy state. We also performed similar experiments on a high-purity [Bmim][BF<sub>4</sub>] material indicating that the anomalous aging is not a result of sample purity issues. We do find that the fragility index decreases for the 99% [Bmim][BF<sub>4</sub>] material relative to the 97% material and that the viscosity itself also increases somewhat.

**Acknowledgment.** The authors would like to thank the American Chemical Society Petroleum Research Fund (grant # 40615-AC7) and the John R. Bradford Endowment at Texas Tech University for supporting this project.

## References and Notes

- (1) Wasserscheid, P.; Welton, T. *Ionic Liquids in Synthesis*; Wiley-VCH: Weinheim, 2003.
- (2) Pereiro, A. B.; Santamarta, F.; Tojo, E.; Rodriguez, A.; Tojo, J. *J. Chem. Eng. Data* **2006**, *51*, 952.
- (3) Fredlake, C. P.; Crosthwaite, J. M.; Hert, D. G.; Aki, S.; Brennecke, J. F. *J. Chem. Eng. Data* **2004**, *49*, 954.
- (4) Ito, N.; Huang, W.; Richert, R. *J. Phys. Chem. B* **2006**, *110*, 4371.
- (5) Ramos, J. J. M.; Afonso, C. A. M.; Branco, L. C. *J. Therm. Anal. Calorim.* **2003**, *71*, 659.
- (6) Rogers, R. D.; Seddon, K. R. *Science* **2003**, *302*, 792.
- (7) Mandanici, A.; Shi, X. F.; McKenna, G. B.; Cutroni, M. *J. Chem. Phys.* **2005**, *122*, 114501.
- (8) Hutcheson, S. A.; McKenna, G. B. *J. Chem. Phys.* **2008**, *129*, 074502-1.
- (9) Richert, R.; Angell, C. A. *J. Chem. Phys.* **1998**, *108*, 9016.
- (10) Angell, C. A.; Ngai, K. L.; McKenna, G. B.; McMillan, P. F.; Martin, S. W. *J. Appl. Phys.* **2000**, *88*, 3113.
- (11) Cox, W. P.; Merz, E. H. *J. Polym. Sci.* **1958**, *28*, 619.
- (12) Ferry, J. *Viscoelastic Properties of Polymers*; Wiley: New York, 1980.
- (13) Larson, R. G. *The Structure and Rheology of Complex Fluids*; Oxford University Press: New York, 1999.
- (14) Cang, H.; Li, J.; Fayer, M. D. *J. Chem. Phys.* **2003**, *119*, 13017.
- (15) Giraud, G.; Gordon, C. M.; Dunkin, I. R.; Wynne, K. *J. Chem. Phys.* **2003**, *119*, 464.
- (16) Rajian, J. R.; Li, S. F.; Bartsch, R. A.; Quitevis, E. L. *Chem. Phys. Lett.* **2004**, *393*, 372.
- (17) Shirota, H.; Funston, A. M.; Wishart, J. F.; Castner, E. W. *J. Chem. Phys.* **2005**, *122*, 184512.
- (18) Noda, A.; Hayamizu, K.; Watanabe, M. *J. Phys. Chem. B* **2001**, *105*, 4603.
- (19) Tokuda, H.; Hayamizu, K.; Ishii, K.; Abu Bin Hasan Susan, M.; Watanabe, M. *J. Phys. Chem. B* **2004**, *108*, 16593.
- (20) Tokuda, H.; Hayamizu, K.; Ishii, K.; Susan, M.; Watanabe, M. *J. Phys. Chem. B* **2005**, *109*, 6103.
- (21) Tsuzuki, S.; Tokuda, H.; Hayamizu, K.; Watanabe, M. *J. Phys. Chem. B* **2005**, *109*, 16474.
- (22) Triolo, A.; Russina, O.; Arrighi, V.; Juranyi, F.; Janssen, S.; Gordon, C. M. *J. Chem. Phys.* **2003**, *119*, 8549.
- (23) Triolo, A.; Russina, O.; Hardacre, C.; Nieuwenhuyzen, M.; Gonzalez, M. A.; Grimm, H. *J. Phys. Chem. B* **2005**, *109*, 22061.
- (24) Wang, Y. T.; Voth, G. A. *J. Phys. Chem. B* **2006**, *110*, 18601.
- (25) Wang, Y. T.; Voth, G. A. *J. Am. Chem. Soc.* **2005**, *127*, 12192.
- (26) Urahata, S. M.; Ribeiro, M. C. C. *J. Chem. Phys.* **2004**, *120*, 1855.
- (27) van Gurp, M.; Palmen, J. *Proc. Int. Congr. Rheol., 10th* **1996**, 134.
- (28) Struik, L. C. E. *Physical Aging in Amorphous Polymers and Other Materials*; Elsevier Scientific Pub. Co.: New York, 1978.
- (29) Marrucci, G. *J. Non-Newtonian Fluid Mech.* **1996**, *62*, 279.
- (30) Mhetar, V.; Archer, L. A. *J. Non-Newtonian Fluid Mech.* **1999**, *81*, 71.
- (31) Bueche, F. *Physical Properties of Polymers*; Interscience Publishers: New York, 1962.
- (32) Earnest, T. R.; Mac knight, W. J. *J. Polym. Sci., Polym. Phys. Ed.* **1979**, *16*, 143.
- (33) Gleissle, W.; Hochstein, B. *J. Rheol.* **2003**, *47*, 897.
- (34) Kulicke, W. M.; Porter, R. S. *Rheol. Acta* **1980**, *19*, 601.
- (35) Ferri, D.; Lomellini, P. *Progr. Trends Rheol. V* **1998**, 385.
- (36) Sui, C. P.; McKenna, G. B. *J. Rheol.* **2007**, *51*, 341.
- (37) Khanna, Y. P. *Polym. Eng. Sci.* **1991**, *31*, 440.
- (38) Vogel, H. *Phys. Z* **1921**, *22*, 645.
- (39) Tammann, G.; Hesse, W. Z. *Anorg. Allg. Chem.* **1926**, *156*, 254.
- (40) Fulcher, G. S. *J. Am. Ceram. Soc.* **1925**, *8*, 339.
- (41) Lubchenko, V.; Wolynes, P. G. *Annu. Rev. Phys. Chem.* **2007**, *58*, 235.
- (42) Angell, C. A. *J. Non-Cryst. Solids* **1991**, *131*, 13.
- (43) Qin, Q.; McKenna, G. B. *J. Non-Cryst. Solids* **2006**, *352*, 2977.
- (44) Debenedetti, P. G. *Metastable Liquids: Concepts and Principles*; Princeton University Press: Princeton, N.J., 1996.
- (45) Moura-Ramos, J. J.; Correia, N. T. *Phys. Chem. Chem. Phys.* **2001**, *3*, 5575.
- (46) Xu, W.; Cooper, E. I.; Angell, C. A. *J. Phys. Chem. B* **2003**, *107*, 6170.
- (47) Leys, J.; Wubbenhorst, M.; Menon, C. P.; Rajesh, R.; Thoen, J.; Glorieux, C.; Nockemann, P.; Thijs, B.; Binnemans, K.; Longuemart, S. *J. Chem. Phys.* **2008**, *128*, 64509.
- (48) Zorn, R.; McKenna, G. B.; Willner, L.; Richter, D. *Macromolecules* **1995**, *28*, 8552.
- (49) Van Gurp, M.; Palmen, J. *Rheol. Bull.* **1998**, *67*, 5.
- (50) Trinkle, S.; Walter, P.; Friedrich, C. *Rheol. Acta* **2002**, *41*, 103.
- (51) Trinkle, S.; Friedrich, C. *Rheol. Acta* **2001**, *40*, 322.
- (52) Clare, B. R.; Bayley, P. M.; Best, A. S.; Forsyth, M.; MacFarlane, D. R. *Chem. Commun.* **2008**, 2689.
- (53) Wilkes, J. S.; Zaworotko, M. J. *J. Chem. Soc.-Chem. Commun.* **1992**, 965.

- (54) Endres, F.; El Abedin, S. Z. *Phys. Chem. Chem. Phys.* **2006**, *8*, 2101.
- (55) Endres, F. *Phys. Chem. Chem. Phys.* **2010**, *12*, 1648.
- (56) Suarez, P. A. Z.; Einloft, S.; Dullius, J. E. L.; de Souza, R. F.; Dupont, J. *J. Chim. Phys. Phys.-Chim. Biol.* **1998**, *95*, 1626.
- (57) Hayes, R.; El Abedin, S. Z.; Atkin, R. *J. Phys. Chem. B* **2009**, *113*, 7049.
- (58) Triolo, A.; Russina, O.; Bleif, H. J.; Di Cola, E. *J. Phys. Chem. B* **2007**, *111*, 4641.
- (59) Triolo, A.; Russina, O.; Fazio, B.; Triolo, R.; Di Cola, E. *Chem. Phys. Lett.* **2008**, *457*, 362.

JP1044089